Journal of Heat and Mass Transfer Research

Journal homepage: https://jhmtr.semnan.ac.ir

Semnan University

ISSN: 2383-3068

Research Article

Environmental, Economic and Exergy Analysis of a Parabolic Trough Solar Collector with Finned Absorber Tube

Farhad Vahidinia [a], Alireza Aghaei [b]*, Hossein Khorasanizadeh [b]

[a] *Department of Mechanical Engineering, Faculty of Engineering, University of Zabol, Zabol, Iran*

[b] *Faculty of Mechanical Engineering, University of Kashan, Kashan, Iran*

ARTICLE INFO

Article history:

Received: 2024-05-26

Revised: 2024-09-28

Accepted: 2024-09-28

Keywords:

Economic analysis;

Energy;

Environmental analysis;

Hybrid nanofluid;

Parabolic solar collector;

ABSTRACT

Considering the excellent properties of hybrid nanofluids, it is a good idea to use them to improve the performance of solar collectors. The performance of a parabolic trough solar collector equipped with an internally finned absorber tube (IFAT) has been numerically studied based on the environmental, economic, exergy and energy perspectives. The working fluid of the collector is hybrid nanofluid (HNF) consists of MWCNT and Fe_3O_4 nanoparticles and Therminol VP-1 as base fluid (BF). The volume fraction of nanoparticles is 3%, the operating fluid temperature is 600 K and the Reynolds number is in the range of 2×10^4-2×10^5. The fluid flow is simulated using Ansys-Fluent software. Environmental analysis was done using the life cycle method, and economic analysis was based on the levelized cost of energy. Investigation of the results showed that the energy and exergy efficiencies of the collector when using the IFAT is higher than the smooth absorber tube (SAT) and using HNF is higher the base fluid. The maximum energy efficiency enhancement of the PTC using IFAT-BF, SAT-HNF and IFAT-HNF compared to SAT-BF is 4.93, 1.49 and 5.35%, respectively and the maximum exergy efficiency enhancement is 6.09, 1.6 and 6.6%, respectively. Based on the economic approach, it was observed that for the Re lower than 5×10^4, the use of PTC with IFAT is more economical than the PTC with SAT. The environmental analysis showed that the use of the PTC with SAT compared to PTC with IFAT and also the use of HNF instead of the BF produces less CO_2 in the life cycle of the collector.

1. Introduction

Nowadays, the use of solar energy in various applications is expanding [1,2]. Parabolic trough solar collectors (PTCs) play an important role in the production of electricity using solar energy. Studies show that more than 90% of electricity produced using solar thermal systems is related to the PTCs [3]. The operating fluid of these types of collectors is thermal oils [4]. Water and steam can also be used as the working fluid, and molten salts can also be used for temperatures up to 600 °C [5]. In PTCs to achieve higher temperatures, liquid metals and gaseous fluids can also be used. Although the common use of this type of collector in solar power plants is to generate electricity, they are also used in other applications such as industrial heat production, chemical processes, hydrogen production, and solar absorption refrigeration systems [6].

One of the ways to increase the thermal efficiency of the PTCs is to increase the heat transfer coefficient of the fluid. In the PTC, the sun's radiation is reflected to the receiver after hitting the reflector, and after passing through the cover, it reaches the absorber and finally

* **Corresponding author.**
E-mail address: a.aghaei@kashanu.ac.ir

Cite this article as:
Vahidinia, F., Aghaei, A. and Khorasanizadeh, H., 2025. Environmental, economic and exergy analysis of a parabolic trough solar collector with finned absorber tube. *Journal of Heat and Mass Transfer Research*, 12(1), pp. xx-xx.
https://doi.org/10.22075/JHMTR.2024.39315.2050

reaches the working fluid. Part of the energy absorbed by the absorber is transferred to the fluid, which is useful energy. The higher the heat transfer coefficient, the higher the useful energy input to the working fluid. The amount of heat taken from the absorber tube increases and the absorber tube becomes cooler. Reducing the temperature of the absorber tube reduces the amount of heat loss and subsequently increases the thermal efficiency of the collector. To increase the heat transfer coefficient, several methods such as the use of new working fluids [7] changing the structure of the absorber tube and the use of the turbulator [8] and internal fins [9] have been investigated and studied. These methods of increasing heat transfer are known as passive methods. One of the goals of researchers in recent years has been to use a variety of turbulators such as twisted tape inserts and fins inside the absorber in order to improve the performance of the collector. The turbulators cause better mixing of the flow along the length of the absorber tube. Different twisted tape insert models have been studied for the PTC, including the wavy tape [10], the wall detached twisted tape [11], the spiral wire [12], the helical screw tape [13] and the star flow [14]. These methods in addition to increasing the heat transfer, also increase the friction factor and pressure drop in the fluid, which the latter case is a negative effect on the performance of the collector. Studies show that the amount of pumping power due to the presence of the twisted tape inserts is small compared to the amount of useful energy. Allauddin et al. [15] studied numerically the performance of the roughened PTC. They reported that the performance evaluation criteria (PEC) of the PTC using the absorber tube equipped with circumferential inclined ribs is larger than the dimpled protrusions absorber, and at 500 K and 0.5 kg/s, the PEC in these two cases is 1.46 and 1.18, respectively. Al-Aloosi et al [16] investigated the thermal performance of a PTC by inserting the pin fins with different cross-sections inside the absorber tube. They found that the maximum PEC for circular elliptical and square fins is 1.4, 1.31, and 1.26, respectively.

Considering the extent of nanoscience and its application in various sciences [17,18], the use of nanofluid has also been proposed as an alternative to base fluid [19]. For more than a decade, researchers have conducted extensive studies on the use of nanofluids in solar collectors [20], and most studies have shown that the use of nanofluids has improved the performance of the collectors [21]. Using nanofluid is one of the promising methods to improve the performance of PTCs. Mwesigye et al. evaluated the effect of nanofluids synthetic oil-Al_2O_3 [22] and SWCNTs-Therminol VP-1 [23] on the performance of PTC and showed that the increase in thermal efficiency of the aforementioned nanofluids compared to the base fluid is 7.6% and 4.4%, respectively. The exergy and energy analysis of a PTC using copper nanoparticles in different volume fractions and Syltherm 800 and Therminol VP-1 as base fluids (BFs) was numerically studied by Dou et al. [24]. They illustrated that the maximum enhancement in the exergy and energy efficiencies of the PTC when using Cu-Syltherm 800 instead of thermal oil is 8% and 7.99%, respectively. This enhancement was reported as 2.79 and 2.77% respectively for Cu-Therminol VP-1 instead of the thermal oil. The use of hybrid nanofluids (HNFs) instead of mono nanofluids in solar collectors has improved their performance [25]. HNFs are suitable for use in solar systems due to their excellent properties [26]. Bellos and Tzivanidis [27] reported that the maximum performance of the PTC is found when the collector working fluid is Al_2O_3–TiO_2/Syltherm 800 HNF. In another study, two HNFs of Al_2O_3–CuO/Syltherm 800 and Al_2O_3–CeO_2/Syltherm 800 were used by Al-Oran et al [28] to evaluate the performance of PTC and it was concluded that the highest performance was obtained using Al_2O_3–CeO_2/Syltherm 800. Khan et al. [29] studied the effect of MWCNT–TiO_2/Therminol VP-1 on the performance of a PTC in two converging-diverging and smooth absorbers. They reported that the enhancement in energy efficiency of PTC using HNFs compared to the BF for smooth absorber tube (SAT) was between 1.70% and 1.91% and for that of convergent-divergent between 3.61% and 5.27%. Vahidinia et al [30] evaluated the energy, exergy and environmental performance of a PTC using Al_2O_3/SiO_2-Syltherm 800 HNF. They showed that the exergy and energy efficiencies of the collector when using HNF is higher than the BF and mono nanofluid, and the lowest amount of carbon dioxide production during the lifetime of the PTC is achieved when the working fluid is HNF.

In recent years, the simultaneous use of two passive methods of increasing heat transfer in the PTCs has been studied [31]. Improving the performance of the PTC by using nanofluid instead of the BF and by placing the turbulator inside the absorber tube or changing the structure of the absorber tube has led researchers to study the use of both methods instantaneously. In a numerical study, Shaker et al. [32] investigated the performance of the PTC using Al_2O_3-Syltherm 800 and a new flange-shaped turbulator. Their study exhibited that increasing the volume fraction of nanoparticles increases the heat transfer coefficient and makes the temperature of the absorber tube more uniform. Samiezadeh et al. [33] investigated

numerically the energy and hydrodynamic performance of a PTC containing Cu/Al_2O_3-Syltherm 800 HNF by placing the fins in the lower part of the absorber. They reported that at a volume fraction of 2%, the increase in thermal efficiency of the collector using Al_2O_3-Syltherm 800, Al_2O_3-Syltherm 800, and Cu/Al_2O_3-Syltherm 800 compared to the BF is 3.8, 11.3, and 12.2%, respectively. Dezfulizadeh et al. [34] numerically studied the performance of a PTC based on energy, exergy and environmental perspectives using an innovative combined twisted turbulator and HNF. They reported that based on the performance evaluation criteria, the use of HNF is more suitable than the BF. Also, the PEC when using an absorber tube equipped with a turbulator is always greater than 1. On the other hand, their study showed that based on the environmental approach, the PTC when using the HNF produces less carbon dioxide than the BF. Niknejadi et al. [35] numerically investigated the energy, exergy and thermal-hydrodynamic performance of a PTC using a turbulator with different geometrical shapes and Cu-TiO_2/H_2O HNF as the working fluid. The results of their study showed that the PEC when using the turbulator in different geometric is greater than 1. In a numerical study, Pazarlioğlu et al [36] investigated the performance of energy, exergy and entropy generation of a PTC equipped with a dimpled absorber tube containing Al_2O_3/TiO_2-Syltherm 800 HNF. They reported that Nusselt number, entropy generation, exergy efficiency and PEC increase by 38%, and 17.67%, 8.6% and 19.57%, respectively. Hosseini Esfahani et al. [37] evaluated the performance of the PTC based on the energy, exergy, economic and environmental approach by using the combination of two types of twisting band turbulator and wire coil in the absorber tube containing CuO-SWCNT/Water HNF. The results of their study showed that the production rate of environmental pollutants using HNF is lower than the BF. On the other hand, they reported that the energy efficiency, exergy efficiency and PEC using the compound turbulator are lower than the twisted tape turbulator.

Although several studies have been conducted regarding the effect of nanofluids on the performance of the PTC, researchers believe that more studies are needed to determine the exact behavior of nanofluids and their use in these types of collectors [38]. Using the combination of finned absorber tube and HNF in order to improve the performance of the collector is a suitable method that has received less attention. The literature review shows that the performance evaluation of LS-2 PTC with finned absorber tube containing HNF based on the environmental, economic, exergy, and energy approaches with the change of Re and its comparison with the smooth absorber tube has not been done yet, which is important. Based on this, in this study, the performance comparison of the PTC containing MWCNT-Fe_3O_4/Therminol VP-1 HNF in two types of finned and smooth absorber tubes has been done based on the energy, exergy, economic and environmental perspectives. On the other side, the review of last studies shows that in most of them the evaluation of the PTC performance has been studied in the range of low Re. For this purpose, in the present work, the Re is considered in the range of 2×10^4 to 2×10^5. Also, in most of the previous studies related to the combination of HNF and turbulator, water has been used as the BF. Considering that the working fluid of the built power plants equipped with PTCs are mostly thermal oils such as Syltherm 800, Therminol VP-1 and Dowtherm A [39], in this study Therminol VP-1 has been used as the BF.

2. Specifications of the PTC and Numerical solution method

Fig. 1 illustrates the schematic of the receiver of the collector equipped with the IFAT. The upper half of the receiver is exposed to the direct solar heat flux and the lower half is exposed to the reflected solar heat flux from the reflector. The solar radiation after passing through the cover is absorbed by the absorber. The space between the cover and the absorber tube is intended as the vacuum. The dimensions of different components of the collector along with its optical properties as well as solar radiation and environmental conditions are given from [40]. There are 8 fins inside the absorber tube. The length and thickness of each fin are considered 20 mm and 4 mm, respectively, which are located along the length of the absorber. The fins are placed along the length of the absorber.

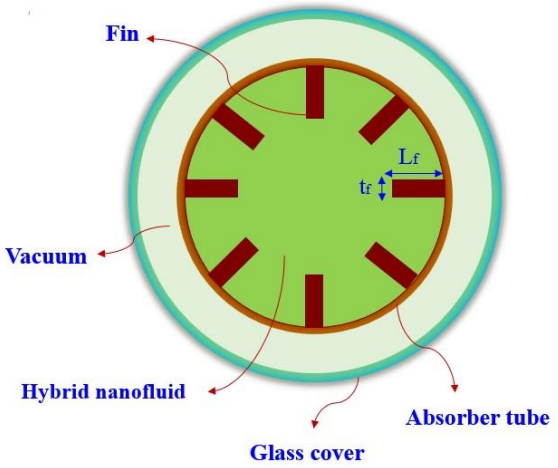

Fig. 1. Schematic of the receiver of the PTC with IFAT

In the numerical simulation, the governing equations of the fluid flow are continuity, momentum and energy. Several assumptions are considered in solving the governing equations. Also, the fluid flow is steady state and three dimensional, and heat generation and external forces are neglected.

The governing equations including the continuity, momentum and energy equations are expressed as follows, respectively [11]:

$$\frac{\partial(\rho u_i)}{\partial x_i} = 0 \ldots \quad (1)$$

$$\frac{\partial}{\partial x_j}(\rho u_i u_j) = \frac{\partial p}{\partial x_i} + \frac{\partial}{\partial x_j}\left(\mu_{eff}\left(\frac{\partial u_i}{\partial x_j} + \frac{\partial u_j}{\partial x_i}\right) - \frac{2}{3}\mu_{eff}\frac{\partial u_i}{\partial x_j}\delta_{ij} - \rho\overline{u_i' u_j'}\right) \quad (2)$$

$$\frac{\partial}{\partial x_j}(\rho u_j c_p T) = \frac{\partial}{\partial x_j}\left(k\frac{\partial T}{\partial x_j} + \frac{\mu_t}{\sigma_{h,t}}\frac{\partial (c_p T)}{\partial x_j}\right) + u_j\frac{\partial p}{\partial x_j} \quad (3)$$

$$\frac{\partial u_i}{\partial x_j}\left(\mu_{eff}\left(\frac{\partial u_i}{\partial x_j} + \frac{\partial u_j}{\partial x_i}\right) - \frac{2}{3}\mu_{eff}\frac{\partial u_i}{\partial x_j}\delta_{ij} - \rho\overline{u_i' u_j'}\right)$$

In this study, in order to model the turbulent flow, the realizable k-ε model is used, and its equations are expressed as [41]:

$$\frac{\partial}{\partial x_j}(\rho k u_j) = \frac{\partial}{\partial x_j}\left((\mu + \frac{\mu_t}{\sigma_k})\frac{\partial k}{\partial x_j}\right) + G_k + \rho\varepsilon \quad (4)$$

$$\frac{\partial}{\partial x_j}(\rho\varepsilon u_j) = \frac{\partial}{\partial x_j}\left(\left(\mu + \frac{\mu_t}{\sigma_k}\right)\frac{\partial \varepsilon}{\partial x_j}\right) + \rho C_1 S\varepsilon \quad (5)$$

$$-\rho C_2\frac{\varepsilon^2}{k + \sqrt{\nu\varepsilon}}$$

Where k represents the turbulent kinetic energy, ε is the rate of dissipation of turbulent kinetic energy and G_k is the production of turbulent kinetic energy, which relationships and more details are provided in [11]. Studies related to the PTCs have shown that among the various k-ε models, the solution results using the realizable k-ε model are more dependable with the experimental results and have higher accuracy [42].

The amount of available radiation at the aperture of PTC is obtained as follows [43]:

$$Q_s = A_a G_b \quad (6)$$

Where G_b is the incident beam irradiation on the collector and A_a is the aperture area of the collector [44]:

$$A_a = (W - D_{co})L \quad (7)$$

The amount of energy absorbed by the absorber is calculated as [27]:

$$Q_{abs} = \eta_{op} Q_s \quad (8)$$

where η_{op} represents the optical efficiency of the PTC and is defined as [43]:

$$\eta_{op} = \rho_m \gamma \tau \alpha K_\theta \quad (9)$$

In which K_θ is the incident angle modifier [45].

The useful energy output from the PTC and received by the fluid is calculated through the following equation [46]:

$$Q_u = \dot{m} c_p (T_{out} - T_{in}) \quad (10)$$

The energy efficiency of the PTC is calculated based on the following [30]:

$$\eta_{en} = \frac{Q_u}{Q_s} \quad (11)$$

The heat transfer coefficient of the working fluid is defined as [30]:

$$h = \frac{Q_u}{\pi D_{ri} L(T_r - T_{fm})} \quad (12)$$

The average temperature of the working fluid is expressed as [44]:

$$T_{fm} = \frac{T_{out} + T_{in}}{2} \quad (13)$$

The Nusselt number is calculate as [47]:

$$Nu = \frac{hD_{ri}}{\lambda} \quad (14)$$

The pressure drop of the working fluid along the absorber tube (Pa) is calculated according to the following:

$$\Delta p = p_{ave,in} - p_{ave,out} \quad (15)$$

The friction factor is calculated as [48]:

$$f = \frac{2\Delta p D_{ri}}{\rho u_m^2 L} \quad (16)$$

The Reynolds number is expressed as [49]:

$$Re = \frac{\rho u_m D_{ri}}{\mu} \quad (17)$$

The cover is exposed to thermal losses due to radiation from the sky and environmental convections losses. The simulation of these losses in the software is done by defining the sky temperature and the heat transfer coefficient between the cover and the surrounding. Based on this, the sky temperature [50] and the heat transfer coefficient between the cover and the environment [51] are expressed by the following relations, respectively.

$$T_{sky} = 0.0552 {T_{amb}}^{1.5} \quad (18)$$

$$h_{out} = 4 {V_w}^{0.58} {D_{co}}^{-0.42} \quad (19)$$

Two sides of this space will be assumed to be symmetrical [52]. The emissivity of the cover is 0.86, and the emissivity of the absorber is assumed to be the function of the absorber temperature and is expressed as [53].

$$\varepsilon_r = 0.062 + 2 \times 10^{-7}(T_r - 273.15) \quad (20)$$

Solar exergy is calculated through the Petela relation [54]:

$$E_s = Q_s\left(1 - \frac{4}{3}\frac{T_{amb}}{T_{sun}} + \frac{1}{3}\left(\frac{T_{amb}}{T_{sun}}\right)^4\right) \quad (21)$$

The useful exergy of the working flow is defined as [40]:

$$E_u = Q_u - \dot{m}c_p T_{amb} \ln\left(\frac{T_{out}}{T_{in}}\right) - \dot{m}T_{amb}\frac{\Delta p}{\rho T_{fm}} \quad (22)$$

The exergy efficiency of the collector is calculated as [55]:

$$\eta_{ex} = \frac{E_u}{E_s} \quad (23)$$

Due to the fact that in the present work, the performance of PTC is evaluated with two types of smooth and fined absorber tubes HNFs, three criteria of hydrodynamic- thermal performance evaluation are used for comparison. Performance evaluation criteria under constant pumping power (PEC I), under constant pressure drop (PEC II) and under constant flow rate (PEC III) are defined as [56,57]:

$$PECI = \frac{Nu_{finned}/Nu_{smooth}}{(f_{finned}/f_{smooth})^{\frac{1}{3}}} \quad (24)$$

$$PECII = \frac{Nu_{finned}/Nu_{smooth}}{(f_{finned}/f_{smooth})^{\frac{1}{2}}} \quad (25)$$

$$PECIII = \frac{Nu_{finned}/Nu_{smooth}}{f_{finned}/f_{smooth}} \quad (26)$$

For economic estimation, the following relation is used. In this regard, the economic analysis is only evaluated based on the investment cost of the collector and the change in its structure [58].

$$LCOE = \frac{CO}{\eta_{en} Q_s N} \quad (27)$$

Where LCOE is the levelized cost of energy, CO indicates the cost of the collector, and N is the number of operating hours of the system.

The amount of carbon dioxide is estimated according to the life cycle method based on the following relation [40].

$$CO_2 = y_{CO_2} Q_u N_h N_d N_y \quad (28)$$

where CO2 is the amount of carbon dioxide emission (kg), yCO_2 is the estimated coefficient of carbon dioxide emission for solar collectors (kg/Wh) and Nh, Nd and Ny are the number of hours of daily operation of the PTC, the number of sunny days in a year and the number of years of operation of the collector in the life cycle, respectively.

In order to calculate the amount of CO_2 when using HNF instead of the BF, the aperture area reduction approach has been applied. For calculating the aperture area the following equation is used [40].

$$A_c = \frac{\dot{m}c_p(T_{out} - T_{in})}{\eta_{en} G_b} \quad (29)$$

In the present study, Therminol VP-1 was used as the BF. The thermophysical properties of Therminol VP-1 including density, ρ_{bf} (kg/m^3), the specific heat capacity, cpbf (J/kg.K), thermal conductivity, λ_{bf} (W/m.K) and dynamic viscosity, μ_{bf} (mPa.s) as a function of temperature are defined according to the following equations [3].

$$\rho_{bf} = 1.4386 \times 10^3 - 1.8711T + 2.737 \times 10^{-3}T^2 - 2.3793 \times 10^{-6}T^3 \quad (30)$$

$$cp_{bf} = 2.125 \times 10^3 - 11.017T + 0.049862T^2 - 7.7663 \times 10^{-5}T^3 + 4.394 \times 10^{-8}T^4 \quad (31)$$

$$\lambda_{bf} = 0.14644 + 2.0353 \times 10^{-5}T - 1.9367 \times 10^{-7}T^2 + 1.0614 \times 10^{-11}T^3 \quad (32)$$

$$\mu_{bf} = 23.165 - 0.1476T + 3.617 \times 10^{-4}T^2 - 3.9844 \times 10^{-7}T^3 + 1.6543 \times 10^{-10}T^4 \quad (33)$$

Where ρ_{bf}, cp_{bf} and λ_{bf} are presented for 285.15 (K) ≤ T ≤ 698.15 (K) and μ_{bf} is given for 373.15 (K) ≤ T ≤ 698.15 (K).

In this article, two nanoparticles of Fe_3O_4 and MWCNT are used in HNF. The properties of nanocomposite of MWCNT–Fe_3O_4 are calculated through the following equations, where the number of 1 means nanoparticle Fe_3O_4 and the number of 2 means nanoparticle MWCNT [7].

$$\phi = \phi_1 + \phi_2 \quad (34)$$

$$\rho_{np} = \frac{\phi_1\rho_{np,1} + \phi_2\rho_{np,2}}{\phi} \quad (35)$$

$$cp_{np} = \frac{\phi_1 cp_{np,1} + \phi_2 cp_{np,2}}{\phi} \quad (36)$$

$$\lambda_{np} = \frac{\phi_1\lambda_{np,1} + \phi_2\lambda_{np,2}}{\phi} \quad (37)$$

The density of HNF is calculated as [59]:

$$\rho_{nf} = (1 - \phi)\rho_{bf} + \phi\rho_{np} \quad (38)$$

The specific heat capacity of HNF is expressed as [60].

$$cp_{nf} = \frac{(1 - \phi)\rho_{bf} cp_{bf} + \phi\rho_{np} cp_{np}}{\rho_{nf}} \quad (39)$$

The thermal conductivity of HNF as [61]:

$$\lambda_{nf} = \lambda_{bf}\frac{\lambda_{np} + (\Gamma-1)\lambda_{bf} + (\Gamma-1)(\lambda_{np}-\lambda_{bf})\phi}{\lambda_{np} + (\Gamma-1)\lambda_{bf} - (\lambda_{np}-\lambda_{bf})\phi} \quad (40)$$

The dynamic viscosity of HNF is defined as [62].

$$\mu_{nf} = \frac{\mu_{bf}}{(1-\phi)^{2.5}} \quad (41)$$

In order to simulate the heat flux on the absorber tube wall, the following relations are used, which show the heat fluxes on the lower and upper walls, respectively.

$$q''_{up,wall} = \tau G_b \quad (42)$$

$$q''_{down,wall} = \eta_{op} C_R G_b \quad (43)$$

Where C_R is the concentration ratio of the PTC and is defined as:

$$C_R = \frac{WL}{\frac{1}{2}\pi D_{ro} L} \quad (44)$$

As seen in Fig. 2, the solar heat flux after hitting the cover is absorbed by the upper wall, which is simulated based on Eq. (42). On the other side, the solar heat flux hitting the reflector is reflected towards the lower part of the receiver and after passing through the cover, it hits the lower wall of the absorber, which Eq. (43) is used to simulate it.

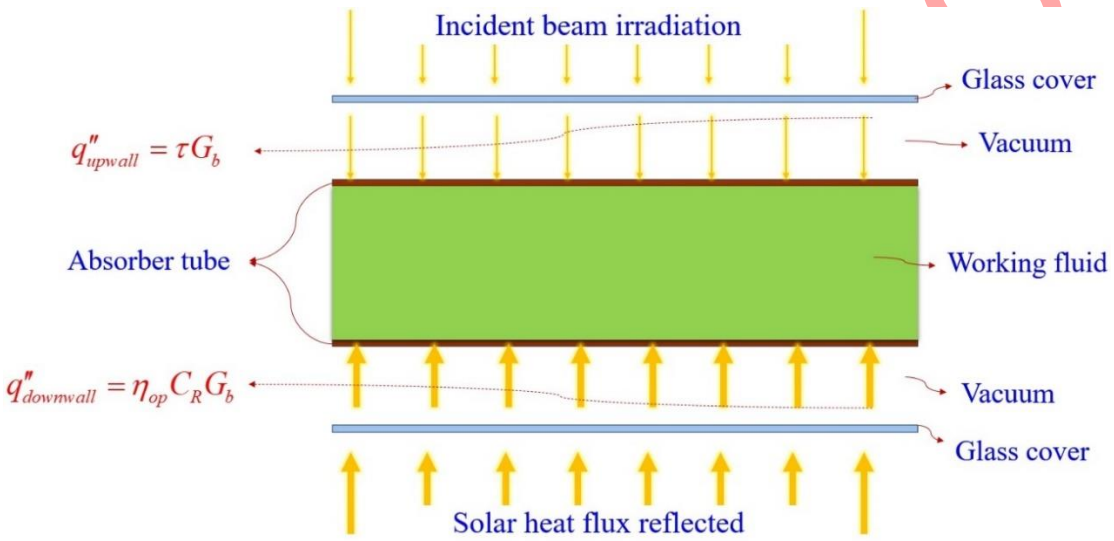

Fig. 2. The solar heat fluxes in the up wall and down wall of the absorber tube

In order to solve the governing equations, Ansys-Fluent software is used, which solves the continuity, momentum, energy equations and the two-equation model of k-ε turbulence based on the finite volume method. Due to the turbulence of the fluid flow, y^+=1 [13]. Fig. 3 shows a sample mesh of the solution domain for the receiver of the PTC equipped with IFAT.

As can be seen in Fig. 3, for consider the effects near the wall of the absorber and the wall of the fins, the boundary layer mesh has also been created. For this purpose, the distance of the first mesh from the wall is calculated as [63]:

$$y = \frac{y^+ \mu}{u_\tau \rho} \quad (45)$$

Where u_τ represents the friction velocity and is calculated based on the following [63]:

$$u_\tau = \sqrt{\frac{\tau_w}{\rho}} \quad (46)$$

In which τ_w is the wall shear stress as:

$$\tau_w = \frac{2}{9}\frac{\rho C_f V^2}{\pi^2 {D_{ri}}^4 10^8} \quad (47)$$

Where C_f is the friction coefficient or the Fanning friction factor that is defined as [64]:

$$C_f = \frac{1}{4}(0.79 ln Re - 1.64)^{-2} \quad (48)$$

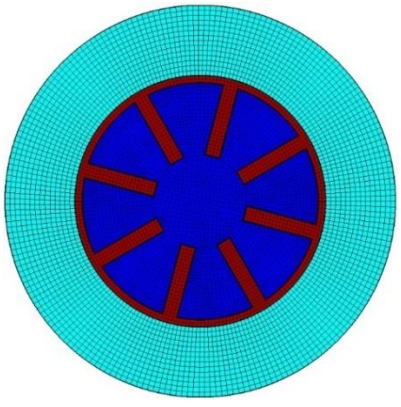

Fig. 3. The sample mesh of the collector equipped with IFAT

In order to design the collector receiver geometry, Design Modeler software was used and Ansys Machining software was used to mesh the geometry. In order to reduce the number of calculations for the SAT, only half of the receiver is meshed. Table 1 presents the optimal number of nodes for both receiver of the PTC equipped with the SAT and IFAT based on the calculation of heat transfer coefficient and pressure drop. As can be seen in Table 1, with the increase in the number of nodes, the deviation between the values of h and ΔP in the secondary state is decreasing compared to the primary state.

Table 1. Investigation of h (W/m2K) and ΔP (Pa) by changing the number of nodes and selecting the best mesh for smooth and finned absorber

absorber	Nodes number	h (W/m²K)	Deviation%	ΔP (Pa)	Deviation%
	434860	1404.6		438	
SAT	1242567	1403.4	-0.085	436.38	-0.370
	1804246	1403.1	-0.021	436.13	-0.057
	1075712	3440.4		2177.3	
IFAT	3202912	3443.6	0.093	2180.3	0.138
	6394313	3444.9	0.038	2181.1	0.037

Experimental results [65] are used in order to validate the accuracy of the output results from Ansys-Fluent software. In Fig. 4, the comparison of the outlet temperature of the working fluid in the numerical solution method with the experimental results of Dudley et al. [65] in 8 different working conditions with different boundary conditions is done for the smooth absorber.

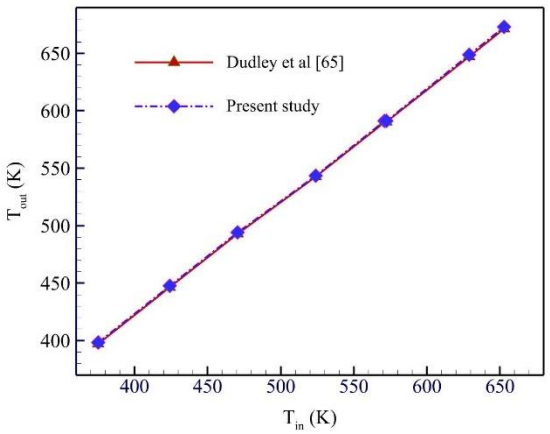

Fig. 4. Comparison of the present study results with experimental results [65]

In this comparison, the solar heat flux is in the range of 880.6 to 982.3 W/m², the inlet fluid temperature is in the range of 375.35 to 652.65 K, the ambient temperature is in the range of 294.35 and 304.25 K, the volumetric flow rate is in the range of 47.7 and 56.8 L/min and the wind speed is in the range of 1 to 4.2 m/s. As shown in Fig. 4, the outlet temperature of the working fluid obtained from the present work and the experimental study [65] is almost the same in all the investigated cases.

3. Results and discussion

In this study, the performance of the PTC with two types of the SAT and the IFAT containing Therminol VP-1 as BF and MWCNT-Fe_3O_4/Therminol VP-1 as HNF is evaluated. The volume fraction of the HNF is 3% and inlet fluid temperature is 600 K. The performance of the collector has been evaluated for 4 cases of smooth absorber tube containing BF, finned absorber tube containing BF, smooth absorber tube containing HNF and finned absorber tube containing HNF for different Re. The Re is considered in the range of 2×10^4 to 2×10^5. Figs. 5 and 6 show the comparison between the temperature of the SAT and the IFAT for BF and HNF, respectively at T= 600 K and Re =2×10^5. According to the temperature contours drawn in Figs. 5 and 6, it can be seen that the temperature of the SAT is higher than the IFAT, and this issue is more evident in the lower part of the absorber tube where there is the concentrated solar heat flux. This shows that the ability of the working fluid in cooling the SAT is lower than the IFAT. In fact, when the working fluid has passed through the finned absorber tube, it has absorbed more heat, or in other words, the useful energy output from the collector is higher in this case. The lower temperature of the absorber tube decreases the amount of radiation loss from the absorber tube to the glass cover. Changing the working fluid and using the HNF instead of the BF slightly decreases the temperature of the absorber tube, which is insignificant at high Re (Figs. 5, 6 and 7).

In Fig. 7, the variation in the difference between the average temperature of the absorber tube and the average temperature of the working fluid in terms of Re is drawn for the SAT and the IFAT. In general, at all ranges of Re,

the temperature difference in the IFAT is lower than the SAT, and this temperature difference is higher at low Re. This means that the working fluid absorbed more heat when leaving the finned absorber tube and reduced the temperature of the absorber. On the other side, with the change of the working fluid, the temperature difference between T_r and T_{fm} changes and it is less for the HNF than the BF, which is more evident in the SAT compare to the IFAT.

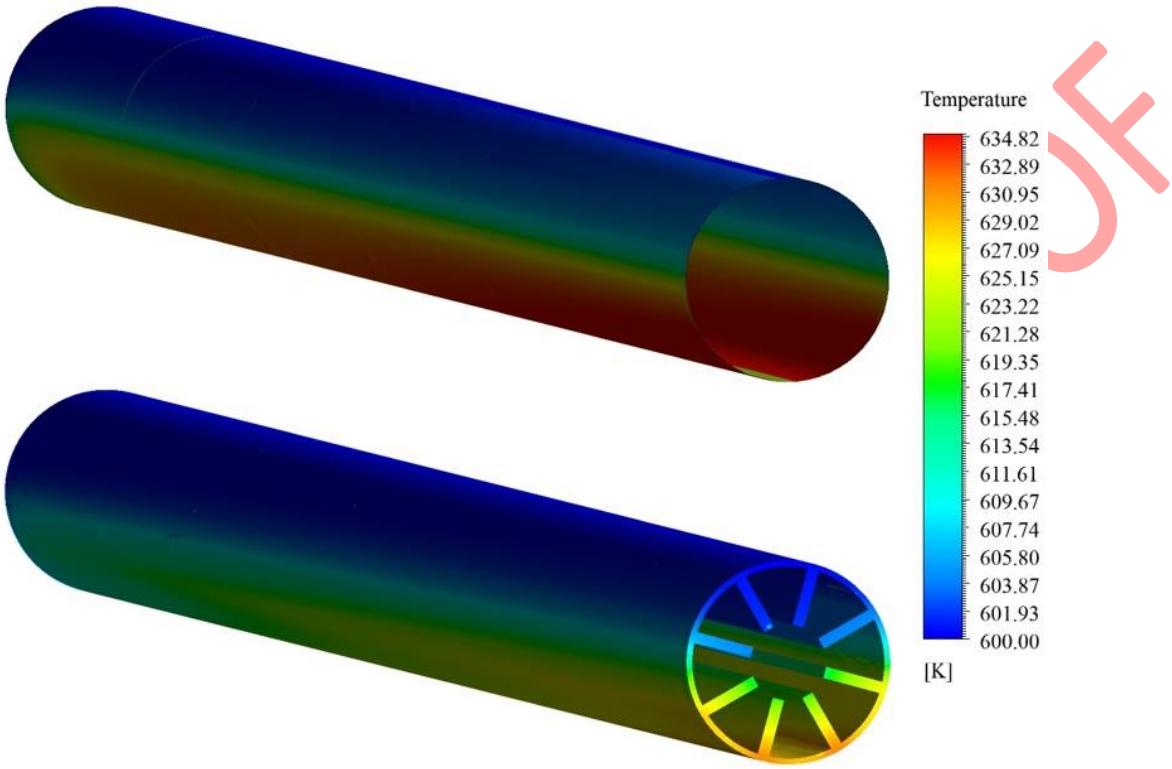

Fig. 5. The temperature of the SAT and the IFAT in the longitudinal direction of the tube at T= 600 K and Re=2×10^5 for the BF

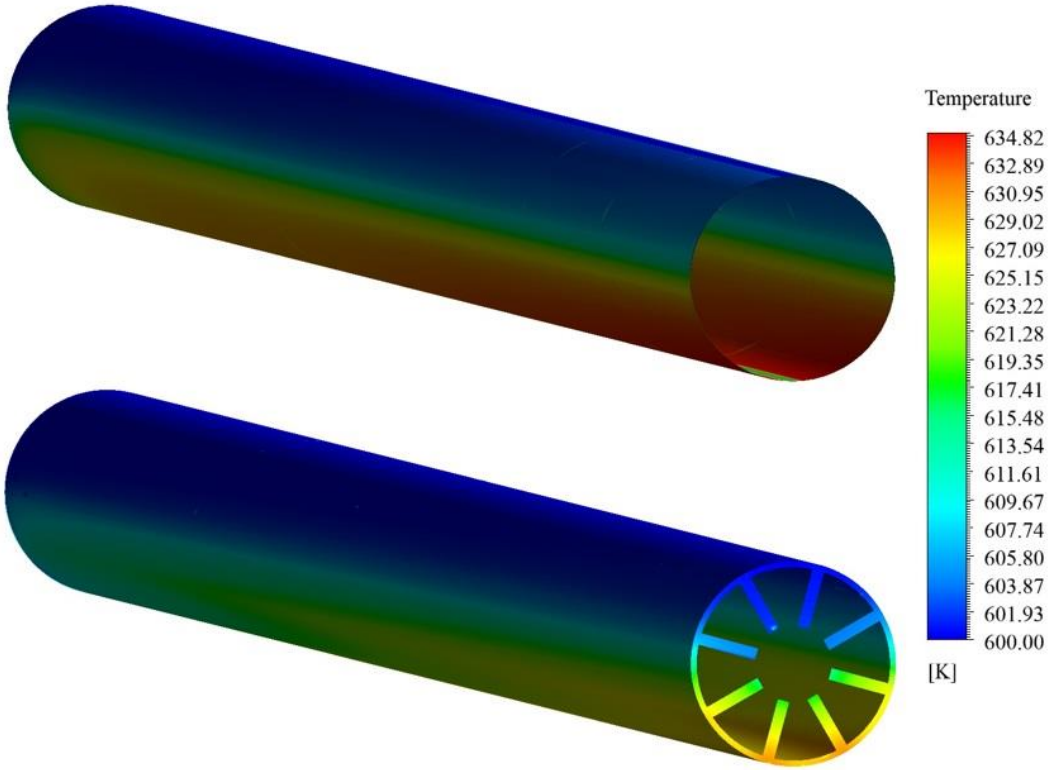

Fig. 6. The temperature of the SAT and the IFAT in the longitudinal direction of the tube at T= 600 K and Re=2×10^5 for the HNF

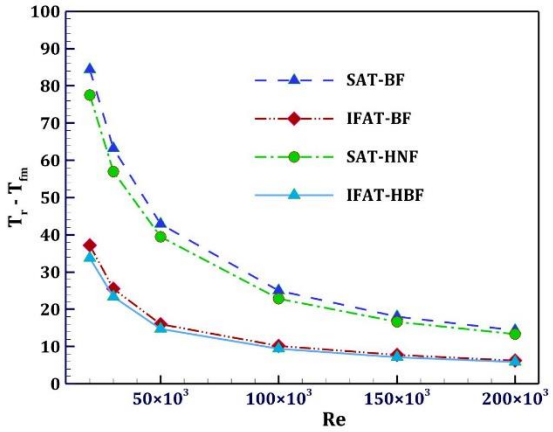

Fig. 7. Variation in the difference between the average temperature of the absorber tube and the average temperature of the working fluid in terms of Re

Fig. 8 shows the contour velocity of the working fluid in the outlet section of the absorber tubes for BF and Fig. 9 illustrates the velocity contour for the HNF. As can be seen in Figs. 8 and 9, the velocity of the working fluid in the IFAT is higher than the SAT. The creation of fins inside the absorber tube increases the flow rate and subsequently increases the disturbances, which also leads to an increase in the convective heat transfer coefficient.

In Fig. 10, the energy efficiency of the PTC is illustrated in terms of Re for the SAT and IFAT using BF and HNF. As it is clear in Fig. 10 for both types of absorber tubes, the energy efficiency of the PTC increases by increasing Re.

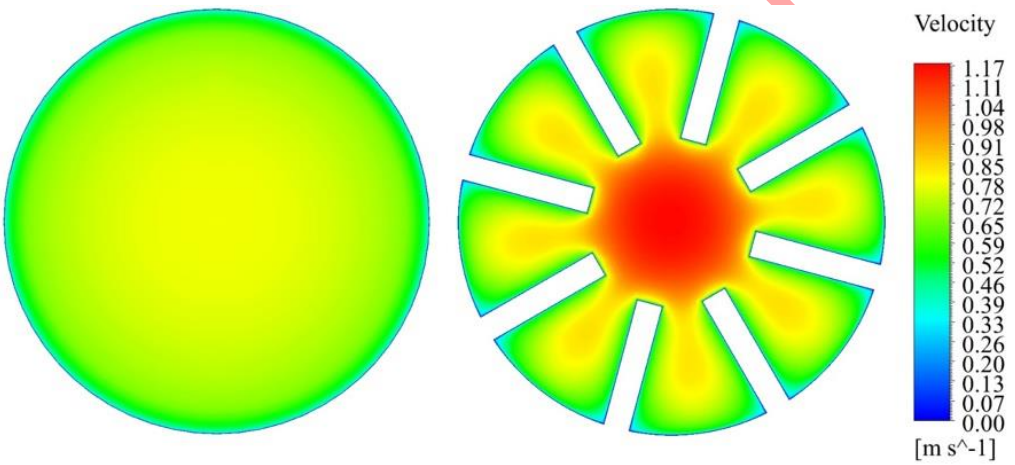

Fig. 8. Fluid outlet velocity contours in the SAT and the IFAT for the BF at $Re=2\times10^5$

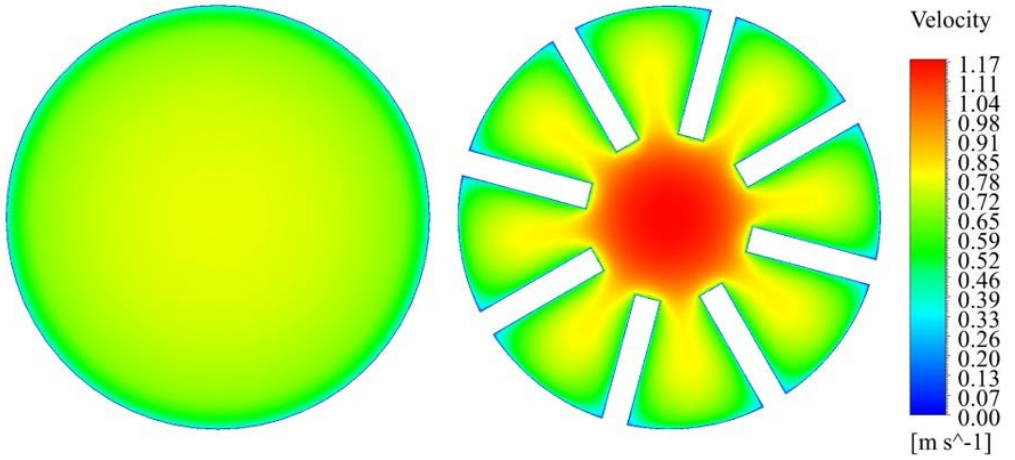

Fig. 9. Fluid outlet velocity contours in the SAT and the IFAT for the HNF at $Re=2\times10^5$

The improvement of energy efficiency is significant at low Re and insignificant at high Re. For example, the enhancement of the energy efficiency by increasing the Re from 2×10^4 to 5×10^4 for the smooth and finned absorber tube is 5.21 and 3.06%, respectively for HNF and 5.77

and 3.34%, respectively for BF. On the other hand, by increasing the Re from 10^5 to 2×10^5 the energy efficiency enhancement is 1.38 and 0.38%, respectively for HNF and 0.76 and 0.32%, respectively for BF. By increasing Re causes disturbances in the fluid flow increases and consequently convective heat transfer coefficient increases, which is shown in Fig. 11. This factor reduces the temperature of the absorber tube and reduces the amount of heat loss and subsequently increases the energy efficiency of the PTC. When the IFAT is used instead of the SAT and HNF instead of the BF, the energy efficiency of the PTC is improved. For $Re=2\times10^4$, The energy efficiency enhancement of the collector with SAT-HNF, IFAT-BF and IFAT-HNF compared to SAT-BF is 1.49, 4.93 and 5.35%, respectively and for $Re=2\times10^5$, it is 0.73, 1.25 and 1.36%, respectively.

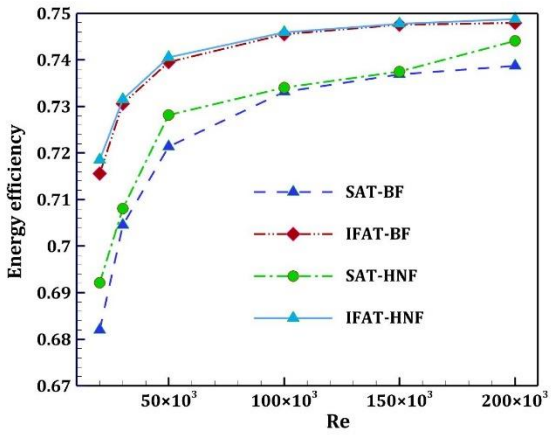

Fig. 10. Variation of the energy efficiency of the PTC with Re for smooth and finned absorber tubes

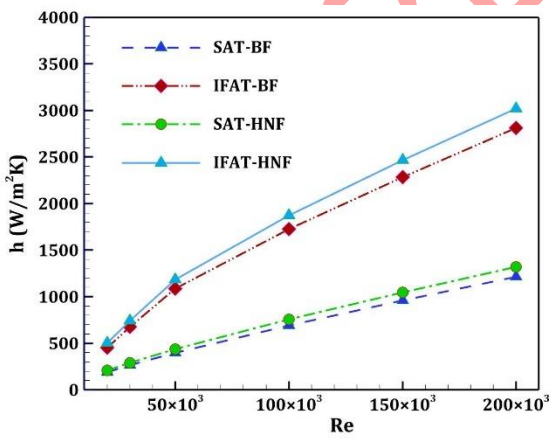

Fig. 11. Variations of the heat transfer coefficient with Re for SAT and IFAT containing BF and HNF

Based on the energy approach, it is more appropriate to use PTCs with the IFAT instead of the SAT and HNF instead of the BF at low Re. When the IFAT is used instead of the SAT, the heat transfer surface increases and subsequently the heat transfer rate between the absorber tube and the working fluid increases. As a result, the heat transfer coefficient of the IFAT is higher than the SAT (Fig. 11). In fact, in the PTC with the IFAT, the larger circumference of the tube and the inner surface of the tube leads to an increase in the convective heat transfer coefficient. Because the heat transfer coefficient increases by increasing the tube circumference [66]. The maximum improvement of the convective heat transfer coefficient of the IFAT compared to the SAT occurs at $Re=5\times10^4$ for BF is 174% and for HNF is 172%. On the other side, according to Fig. 11, it can be seen that the use of HNF instead of BF in both types of absorber tubes increases the convective heat transfer coefficient.

Fig. 12 shows the variation of the Nusselt number in two types of the SAT and the IFAT with Re. As can be seen, in both types of absorber tubes, the Nusselt number increases by increasing the Re. In the internal flow, the increase of Nusselt number by increasing the Re is an obvious issue. The reason for the increase in Nusselt number is the increase in the turbulent nature of the flow with the increase in the Re and the thinning of the thermal boundary layer [60]. On the other hand, according to Fig. 12, using the fin inside the absorber tube and HNF instead of the BF increases the Nusselt number.

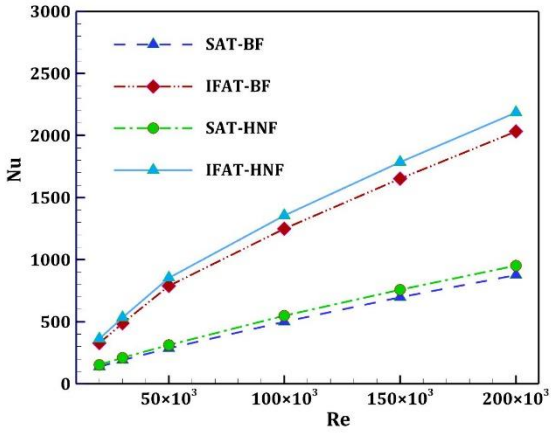

Fig. 12. Variation of the Nusselt number with Re for the SAT and the IFAT

Based on Fig. 10, it was observed that at high Re, the energy efficiency improvement of the collector with the IFAT compared to the SAT is less. On the other side, according to Fig. 11 and Fig. 12, it was observed that for $Re=2\times10^4$ and HNF, the convective heat transfer and the Nusselt number enhancement of the PTC equipped with the IFAT compared to the SAT is 139% and for $Re=2\times10^5$ this enhancement is 132%. The maximum improvement in the heat transfer coefficient of the IFAT compared to the SAT for BF and HNF is 175% and 172%, respectively, which occurs at $Re=5\times10^4$. Therefore, it can be seen that an excessive increase in the Re does not improve the performance of the PTC with the IFAT compared to the SAT. Accordingly,

investigation of the amount of pressure drop in the IFAT at high Re is a necessity.

Fig. 13 shows the variation of pressure drop for the SAT and the IFAT in terms of Re. Based on Fig. 13, it can be seen that increasing the Re increases the pressure drop significantly. For example, by increasing the Re from 2×10^4 to 2×10^5, the amount of pressure drop for the SAT and the IFAT increases by 54 and 47 times, respectively. On the other hand, the use of the IFAT instead of the SAT increases the pressure drop several times. For $Re=2\times10^4$, the pressure drop increase of the IFAT compare to the SAT for BF and HNF is 4.14 and 4.34 times, respectively and for $Re=2\times10^5$, it is 3.54 and 3.73 times, respectively.

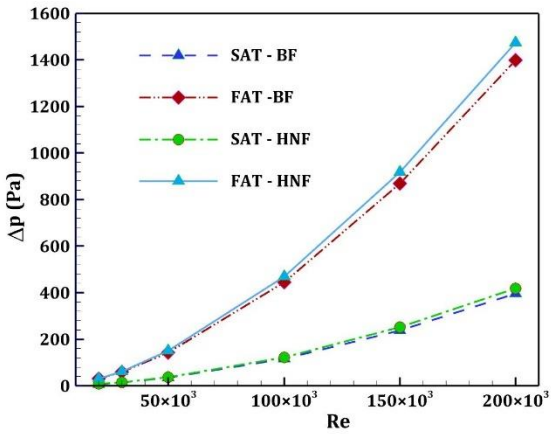

Fig. 13. Variation of the pressure drop with Re for the SAT and the IFAT

One of the parameters that is important to investigate in the heat exchangers is the thermal-hydrodynamic efficiency or the performance evaluation criterion (PEC). Considering that the Nusselt number and the friction factor play a role in defining the PEC, and considering the Nusselt number is investigated in Fig. 14, the friction factor is evaluated in the following. Fig. 14 shows the friction factor of the IFAT and the SAT in terms of Re for BF and HNF. The increasing effect of the Re on the reduction of the friction factor for the IFAT is more than the SAT. By increasing the Re from 2×10^4 to 2×10^5, the reduction of the friction factor for the SAT and the IFAT is 46 and 53%, respectively. On the other side, as illustrated in Fig. 14, the friction factor for the IFAT is much higher than the SAT. The enhancement in the friction factor of the IFAT compared to the SAT is 313% for $Re=2\times10^4$ and 252% for $Re=2\times10^5$. Also, the changes of the friction factor in the SAT and the IFAT with the change of the working fluid are insignificant. The maximum increase in the friction factor of the IFAT compared to the SAT for BF and HNF is 313 and 309%, respectively.

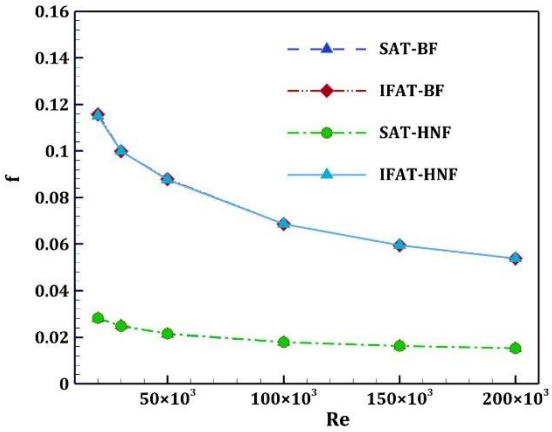

Fig. 14. Variations of the friction factor with the Re for the SAT and the IFAT

Considering the increase in friction factor and Nusselt number in the IFAT compared to the SAT, it can be interesting to investigate the PEC of the PTC. Figs. 15-17 show the PEC of the PTC in three states of constant pumping power (PEC I), constant pressure drop (PEC II) and constant flow rate (PEC III) in terms of the Re versus the IFAT containing the BF, the SAT containing the HNF and the IFAT containing the HNF compare to the SAT containing the BF. According to Figs. 15-17, the values of the PEC I and the PEC II are greater than 1 in all investigated Re. This shows that the use of the IFAT containing the BF and HNF of MWCNT-Fe_3O_4/Therminol VP-1 is more suitable than the SAT. Also, the use of HNF in the SAT is better than the BF.

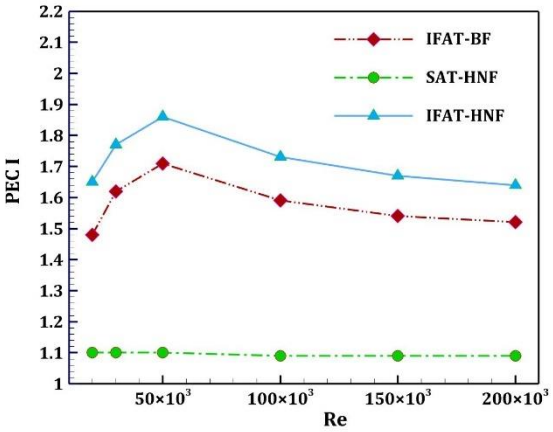

Fig. 15. Variation of the PEC I of the PTC with the Re

On the other hand, as shown in Figs. 15-17, the highest values of the PEC occur at $Re=5\times10^4$. In this case, the values of PEC I for IFAT-BF, SAT-HNF and IFAT-HNF are 1.71, 1.1, and 1.86, respectively and the values of PEC II are 1.35, 1.1, and 1.47, respectively and the values of PEC III is 0.67, 1.1 and 0.73, respectively. Values less than 1 of the PEC III indicate the preference of the PTC with the SAT is better than the IFAT on this criterion. The main reason for this issue is the

significantly higher friction factor of the IFAT compared to the SAT (Eq. (26)). Studies show that comparing the thermal-hydrodynamic performance of solar collectors is often based on the PEC I, and the use of the PEC III is usually not common.

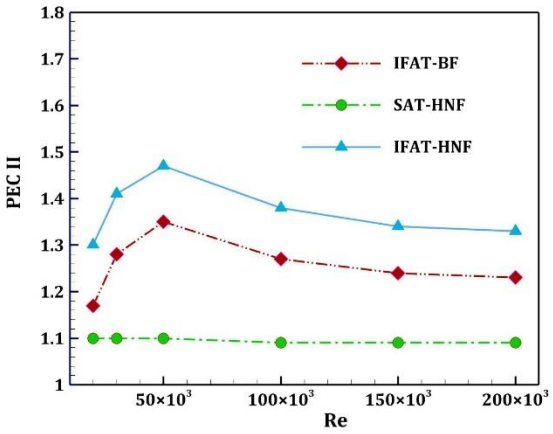

Fig. 16. Variation of the PEC II of the PTC with the Re

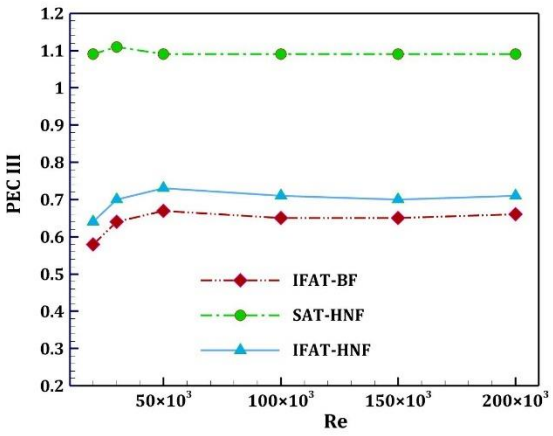

Fig. 17. Variation of the PEC III of the PTC with the Re

In Fig. 18, the pumping power of the PTC for the SAT and the IFAT is drawn. At low Re, the pumping power is almost equal for both types of absorber tubes, but at high Re, the pumping power of the collector with the IFAT is much higher than the SAT. For Re=2×10^5, the pumping power for the IFAT and the SAT is 3 and 1 W, respectively. The reason for the high pumping power of the IFAT compared to the SAT at high Re is the significant pressure drop in the IFAT.

Fig. 19 illustrates the variation of the exergy efficiency of the PTC for the IFAT and the SAT in terms of Re. An increase in the Re at low Re, increases the exergy efficiency, but at high Re, the changes in exergy efficiency are different for the two types of working fluids. On the other side, the exergy efficiency of the PTC with the IFAT is always higher than the SAT and the exergy efficiency by using of HNF is higher than the BF. The enhancement in the exergy efficiency at Re=2×10^4 for the IFAT compared to the SAT for BF and HNF is 6.09 and 4.92%, respectively and at Re=2×10^5 is 1.35 and 0.73%, respectively.

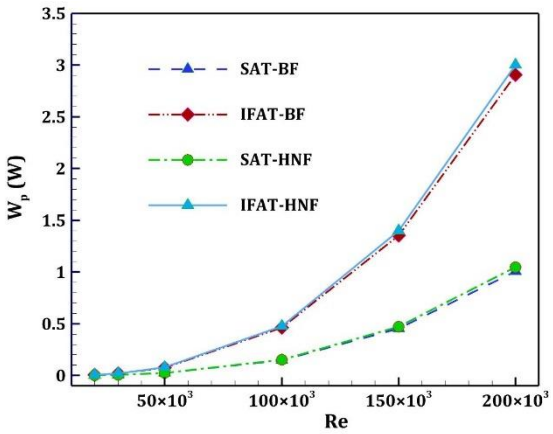

Fig. 18. Variation of the pumping power of the collector for the SAT and the IFAT

On the other hand, the maximum exergy efficiency enhancement of the PTC for SAT-HNF, IFAT-BF and IFAT-HNF compared to SAT-BF is 1.6, 6.09 and 6.6%, respectively. When using the HNF instead of the BF, the exergy performance of the collector is different in two types of absorber tubes. The maximum enhancement in exergy efficiency when using HNF instead of BF in the SAT and the IFAT is 1.6% and 0.48%, respectively. Based on this and as can be seen in Fig. 19, the effect of HNF on the performance of the PTC in the SAT is more than the IFAT.

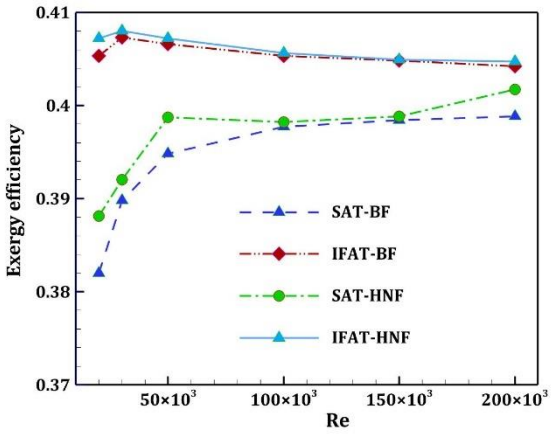

Fig. 19. Variation of the exergy efficiency of the collector for the SAT and the IFAT

Considering that in this research only the investigation of the PTC is considered, the economic analysis is done on this basis. According to the previous studies related to solar collectors, the method of economic evaluation of the collector is based on the estimation of the levelized cost of energy (LCOE) of the system. For the PTC with the SAT, the cost of manufacturing the collector is 200 (Euro/m^2) [58]. If the IFAT is used instead of the SAT, the investment cost will increase by 3% and will be 206 (Euro/m^2) [58].

Also, the number of working hours of the PTC is considered 42000 hours. Fig. 20 shows the LCOE of the PTC for the SAT and the IFAT containing BF and HNF of MWCNT-Fe_3O_4/Therminol VP-1 in different Re. According to Fig. 20, increasing the Re in both types of absorber tubes reduces the LCOE. Also, the severity of LCOE reduction is greater at low Re. By increasing the Re from 2×10^4 to 5×10^4, the LCOE reduction for the smooth absorber and BF, finned absorber and BF, smooth absorber and HNF and finned absorber and HNF is 5.46, 3.23, 5.95 and 2.97%, respectively, and by increasing the Re from 1×10^5 to 2×10^5, it is 0.76, 0.32, 1.36 and 0.38%, respectively. This shows that it is more economical than using the PTC with any type of absorber tube at high Re.

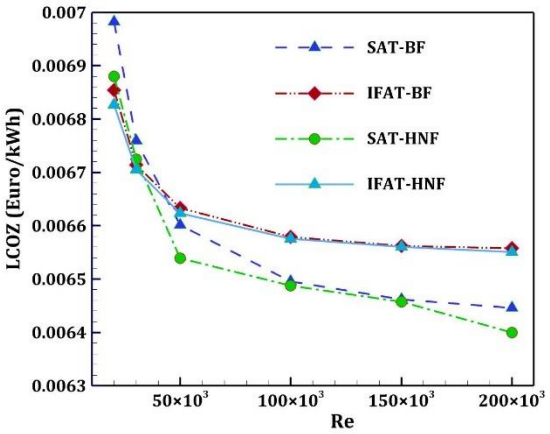

Fig. 20. The LCOE of the PTC with the Re for the finned and smooth absorber tubes

On the other hand, as shown in Fig. 20, for the Re less than 5×10^4, the LCOE is higher when using the SAT than the IFAT. But for the Re greater than 5×10^4, this is vice versa. The enhancement in the LCOE for the SAT compared to the IFAT for the BF and nanofluid is 1.87 and 0.78%, respectively at $Re=2\times10^4$. For $Re=5\times10^4$, the LCOE enhancement of the IFAT compared to the SAT for the BF and HNF is 0.48 and 1.29%, respectively. But for $Re=2\times10^5$, this enhancement is 1.55 and 1.6%, respectively. Therefore, based on the economic approach, the use of the PTC with the IFAT is more suitable than the SAT for Re less than 5×10^4, and the PTC with the SAT is more economical for the Re greater than 5×10^4.

The estimation of the amount of CO_2 in the life cycle of the collector is based on Eq. (28). For this purpose, in this study, the estimated coefficient of CO_2 emission for collectors is 0.00000647 kg/Wh [67], the value of Nh is 7 hours per day, the value of Nd is 300 days per year and the value of Ny is considered 20 years. As seen in Fig. 10, the maximum amount of energy efficiency improvement of the PTC occurs when using the IFAT instead of the SAT at $Re=2\times10^4$. In this case, the volume fraction of nanoparticles is 3% and the fluid inlet temperature is 600 K. Based on this, the environmental analysis of the PTC is performed in the SAT and the IFAT.

Table 2 shows the amount of CO_2 production during the lifetime of the PTC with the SAT and the IFAT for BF and HNF. The values of Table 2 show that the amount of carbon dioxide emission increases when using the IFAT instead of the SAT, and this enhancement for BF and HNF is 348.29 and 421.81 kg, respectively. In fact, according to the life cycle method, using PTC with the IFAT instead of the SAT produces 4.93 and 6.06% more carbon dioxide for BF and HNF as working fluids, respectively. On the other hand, using HNF instead of BF reduces the amount of CO_2, and this amount of reduction is 103.38 and 29.85 kg for the SAT and IFAT, respectively. This shows that based on the environmental analysis using the life cycle method, the use of the SAT instead of the IFAT and using of the HNF instead of the BF in the PTCs is preferable based on the environmental perspective.

Table 2. CO2 emission during the lifetime of the collector for the SAT and the IFAT

	Working fluid	SAT	IFAT
CO_2 produced (kg)	BF	7061.16	7409.45
	HNF	6957.78	7379.6
Reduction of CO_2 produced (kg)		103.38	29.85

4. Conclusions

The objective of this work is to evaluate the performance of the PTC equipped with the SAT and the IFAT containing BF and HNF based on the environmental, exergy, energy and economic perspectives. The Re is in the range of 2×104 to 2×105, the inlet fluid temperature is 600 K, and the volume fraction of nanoparticles is 3%. The analysis of the results exhibited that:

- The temperature of the IFAT is always lower than the SAT in all ranges of Re. Also the temperature difference between the absorber tube and the working fluid at low Re is significant in the SAT compared to those of the IFAT, and by increasing the Re, the variations in the temperature difference in the SAT and the IFAT decreases.
- The maximum enhancement in convective heat transfer coefficient and friction factor of the IFAT compared to the SAT is 175 and 313%, respectively for the BF and 172 and 309%, respectively for the HNF.

- For all the ranges of Re, the exergy and energy efficiencies of the PTC equipped with the IFAT is higher than the SAT, and this issue is more noticeable at low Re.
- The use of HNF instead of the BF increases energy and exergy efficiencies, which is more evident in the SAT.
- The maximum amount of PEC I, PEC II and PEC III when using the IFAT instead of the SAT is 1.71, 1.36, and 0.76, respectively. These values are obtained by using HNF and compared to the basic state, i.e. SAT-BF. However, when using SAT-HNF, the highest values of PECs are almost 1.1.
- According to the economic analysis, for Re less than 5×104, the use of the IFAT is more economical than the SAT, and for Re higher than 5×104, the use of the SAT is more economical.
- Based on the environmental analysis, it is more appropriate to use the SAT compare to the IFAT and the HNF compared to BF in the PTCs.

Nomenclature

A_a	Aperture area (m^2)
c_p	Specific heat capacity (J/kgK)
D_{ci}	Cover inner diameter (m)
D_{co}	Cover outer diameter (m)
D_{ri}	Receiver inner diameter (m)
G_b	Incident solar beam irradiation (W/m^2)
L	Length (m)
$\dot{m}$	Mass flow rate (kg/s)
p	Pressure (Pa)
Q	Heat flux (W)
T	Temperature (K)
u	Velocity (m/s)
V	Volumetric flow rate (L/min)
W	Width (m)

Greek letters

α	Absorptivity of the absorber tube
ε	Emissivity
η	Efficiency
k	Thermal conductivity (W/m K)
μ	Dynamic viscosity (Pa s)
ρ	density (kg/m^3)
σ	Stefan Boltzmann's constant (W/m^{2}K^4)
τ	transmissivity for the cover

Subscripts

a	Aperture
amb	Ambient
b	Beam
c	Cover
ci	Inner cover
co	Outer cover
ex	Exergy
in	Inlet
loss	Heat loses
op	Optical
out	Outlet
r	Receiver
ri	Inner receiver
th	Thermal
u	Useful
w	Wind

Abbreviations

CO	Cost of the collector
LCOE	Levelized cost of energy
PEC	Performance evaluation criteria
PTCs	Parabolic trough collectors

Acknowledgments

Farhad Vahidinia would like to thank the University of Zabol for providing financial support (Grant code. IR-UOZ-GR-6592).

References

[1] Hamzah, H., Hasan, S.I., Küçüka, S., 2020. Numerical study of thermal transport in a flat-plate solar collector using novel absorber plate, in: Environmentally-Benign Energy Solutions. Springer, pp. 649–662.

[2] Pazarlioğlu, H.K., Ekiciler, R., Arslan, K., 2021. Numerical analysis of effect of impinging jet on cooling of solar air heater with longitudinal fins. Heat Transf. Res. 52.

[3] Mwesigye, A., Huan, Z., Meyer, J.P., 2016b. Thermal performance and entropy generation analysis of a high concentration ratio parabolic trough solar collector with Cu-Therminol® VP-1 nanofluid. Energy Convers. Manag. 120, 449–465.

[4] Bellos, E., Tzivanidis, C., 2019. Alternative designs of parabolic trough solar collectors. Prog. Energy Combust. Sci. 71, 81–117.

[5] Myers Jr, P.D., Goswami, D.Y., 2016. Thermal energy storage using chloride salts and their eutectics. Appl. Therm. Eng. 109, 889–900.

[6] Bellos, E., Tzivanidis, C., Said, Z., 2020. A systematic parametric thermal analysis of nanofluid-based parabolic trough solar collectors. Sustain. Energy Technol. Assessments 39, 100714.

[7] Ekiciler, R., Arslan, K., Turgut, O., Kurşun, B., 2020. Effect of hybrid nanofluid on heat transfer performance of parabolic trough solar collector receiver. J. Therm. Anal. Calorim.

[8] Akbarzadeh, S., Valipour, M.S., 2020. Energy and exergy analysis of a parabolic trough collector using helically corrugated absorber tube. Renew. Energy 155, 735–747.

[9] Vahidinia, F., 2024. Evaluation of energy and exergy of a parabolic trough solar collector equipped with internal fin and star turbulator absorber tube. J. Appl. Comput. Sci. Mech. 36, 97–114. https://doi.org/10.22067/jacsm.2023.83484.1199

[10] Zhu, X., Zhu, L., Zhao, J., 2017. Wavy-tape insert designed for managing highly concentrated solar energy on absorber tube of parabolic trough receiver. Energy 141, 1146–1155.

[11] Mwesigye, A., Bello-Ochende, T., Meyer, J.P., 2016a. Heat transfer and entropy generation in a parabolic trough receiver with wall-detached twisted tape inserts. Int. J. Therm. Sci. 99, 238–257.

[12] Şahin, H.M., Baysal, E., Dal, A.R., Şahin, N., 2015. Investigation of heat transfer enhancement in a new type heat exchanger using solar parabolic trough systems. Int. J. Hydrogen Energy 40, 15254–15266.

[13] Song, X., Dong, G., Gao, F., Diao, X., Zheng, L., Zhou, F., 2014. A numerical study of parabolic trough receiver with nonuniform heat flux and helical screw-tape inserts. Energy 77, 771–782.

[14] Bellos, E., Tzivanidis, C., 2018a. Investigation of a star flow insert in a parabolic trough solar collector. Appl. Energy 224, 86–102.

[15] Allauddin, U., Rafique, M.U., Malik, O., Rashid, O., Waseem, A., King, P., Karim, M., Almond, H., 2023. Investigation of the Thermo-hydraulic performance of a roughened Parabolic trough collector. Appl. Therm. Eng. 219, 119523.

[16] Al-Aloosi, W., Alaiwi, Y., Hamzah, H., 2023. Thermal performance analysis in a parabolic trough solar collector with a novel design of inserted fins. Case Stud. Therm. Eng. 49, 103378.

[17] Hamzah, H., Albojamal, A., Sahin, B., Vafai, K., 2021. Thermal management of transverse magnetic source effects on nanofluid natural convection in a wavy porous enclosure. J. Therm. Anal. Calorim. 143, 2851–2865.

[18] Majidi, M., Bijarchi, M.A., Arani, A.G., Rahimian, M.H., Shafii, M.B., 2022. Magnetic field-induced control of a compound ferrofluid droplet deformation and breakup in shear flow using a hybrid lattice Boltzmann-finite difference method. Int. J. Multiph. Flow 146, 103846.

[19] Vahidinia, F., Rahmdel, M., 2015. Turbulent mixed convection of a nanofluid in a horizontal circular tube with non-uniform wall heat flux using a two-phase approach. Challenges Nano Micro Scale Sci. Technol. 3, 106–117.

[20] Farzaneh, H., Behzadmehr, A., Samimi, A., 2021. Stability of Nanofluid-Surfactants as Volumetric Receivers in Parabolic Trough Solar Collectors; a Molecular Dynamic Approach. Challenges Nano Micro Scale Sci. Technol. 9, 109–116.

[21] Ekiciler, R., Arslan, K., Turgut, O., 2023. Application of nanofluid flow in entropy

generation and thermal performance analysis of parabolic trough solar collector: experimental and numerical study. J. Therm. Anal. Calorim. 148, 7299–7318.

[22] Mwesigye, A., Huan, Z., Meyer, J.P., 2015. Thermodynamic optimisation of the performance of a parabolic trough receiver using synthetic oil–Al_2O_3 nanofluid. Appl. Energy 156, 398–412.

[23] Mwesigye, A., Yılmaz, İ.H., Meyer, J.P., 2018. Numerical analysis of the thermal and thermodynamic performance of a parabolic trough solar collector using SWCNTs-Therminol®VP-1 nanofluid. Renew. Energy 119,844–862. https://doi.org/10.1016/j.renene.2017.10.047

[24] Dou, L., Ding, B., Zhang, Q., Kou, G., Mu, M., 2023. Numerical investigation on the thermal performance of parabolic trough solar collector with synthetic oil/Cu nanofluids. Appl. Therm. Eng. 227, 120376.

[25] Nabi, H., Pourfallah, M., Gholinia, M., Jahanian, O., 2022. Increasing heat transfer in flat plate solar collectors using various forms of turbulence-inducing elements and CNTs-CuO hybrid nanofluids. Case Stud. Therm. Eng. 33, 101909.

[26] Ahmadi, M.H., Ghazvini, M., Sadeghzadeh, M., Nazari, M.A., Ghalandari, M., 2019. Utilization of hybrid nanofluids in solar energy applications: a review. Nano-Structures & Nano-Objects 20, 100386.

[27] Bellos, E., Tzivanidis, C., 2018b. Thermal analysis of parabolic trough collector operating with mono and hybrid nanofluids. Sustain. Energy Technol. Assessments 26, 105–115.

[28] Al-Oran, O., Lezsovits, F., Aljawabrah, A., 2020. Exergy and energy amelioration for parabolic trough collector using mono and hybrid nanofluids. J. Therm. Anal. Calorim. 1–18.

[29] Khan, M.S., Abid, M., Yan, M., Ratlamwala, T.A.H., Mubeen, I., 2021. Thermal and thermodynamic comparison of smooth and convergent-divergent parabolic trough absorber tubes with the application of mono and hybrid nanofluids. Int. J. Energy Res. 45, 4543–4564.

[30] Vahidinia, F, Khorasanizadeh, H., Aghaei, A., 2021. Comparative energy, exergy and CO_2 emission evaluations of a LS-2 parabolic trough solar collector using Al_2O_3/SiO_2-Syltherm 800 hybrid nanofluid. Energy Convers. Manag. 245, 114596.

[31] Aliehyaei, M., Joshaghani, A.H., Najafizadeh, M.M., 2023. Energy, exergy, economic and environmental analysis of parabolic trough collector containing hybrid nanofluid equipped with turbulator. Eng. Anal. Bound. Elem. 150, 492–506.

[32] Shaker, B., Gholinia, M., Pourfallah, M., Ganji, D.D., 2022. CFD analysis of Al_2O_3-sylltherm oil Nanofluid on parabolic trough solar collector with a new flange-shaped turbulator model. Theor. Appl. Mech. Lett. 12, 100323.

[33] Samiezadeh, S., Khodaverdian, R., Doranehgard, M.H., Chehrmonavari, H., Xiong, Q., 2022. CFD simulation of thermal performance of hybrid oil-Cu-Al_2O_3 nanofluid flowing through the porous receiver tube inside a finned parabolic trough solar collector. Sustain. Energy Technol. Assessments 50, 101888.

[34] Dezfulizadeh, A., Aghaei, A., Sheikhzadeh, G.A., 2023. Comprehensive 3E analyses of a parabolic trough collector equipped with an innovative combined twisted turbulator. Eng. Anal. Bound. Elem. 150, 507–527.

[35] Niknejadi, M., Alizadeh, A. ad, Zekri, H., Ruhani, B., Nasajpour-Esfahani, N., Smaisim, G.F., 2023. Numerical simulation of the thermal-hydraulic performance of solar collector equipped with vector generators filled with two-phase hybrid nanofluid Cu-TiO2/H2O. Eng. Anal. Bound. Elem. 151, 670–685.

[36] Pazarlıoğlu, H.K., Ekiciler, R., Arslan, K., Mohammed, N.A.M., 2023a. Exergetic, Energetic, and entropy production evaluations of parabolic trough collector retrofitted with elliptical dimpled receiver tube filled with hybrid nanofluid. Appl. Therm. Eng. 223, 120004.

[37] Hosseini Esfahani, A., Aliehyaei, M., Hassani Joshaghani, A., Najafizadeh, M.M., 2023. Economic, Exergy, and Environmental Analyses of Parabolic Trough Solar Collector with Turbulator Containing Polymer Hybrid Nanofluid. Eng. Energy Manag. 12, 80–99.

[38] Gupta, S.K., 2023. A short & updated review of nanofluids utilization in solar parabolic trough collector. Mater. Today Proc.

[39] Aqachmar, Z., Allouhi, A., Jamil, A., Gagouch, B., Kousksou, T., 2019. Parabolic trough solar thermal power plant Noor I in Morocco. Energy 178, 572–584.

[40] Vahidinia, F, Khorasanizadeh, H., Aghaei, A., 2023. Energy, exergy, economic and environmental evaluations of a finned

absorber tube parabolic trough collector utilizing hybrid and mono nanofluids and comparison. Renew. Energy 205, 185–199.

[41] Mwesigye, A., Bello-ochende, T., Meyer, J.P., 2013. Numerical investigation of entropy generation in a parabolic trough receiver at different concentration ratios. Energy 53, 114–127. https://doi.org/10.1016/j.energy.2013.03.006

[42] Huang, Z., Yu, G.L., Li, Z.Y., Tao, W.Q., 2015. Numerical study on heat transfer enhancement in a receiver tube of parabolic trough solar collector with dimples, protrusions and helical fins. Energy Procedia 69, 1306–1316.

[43] Vahidinia, Farhad, Khorasanizadeh, H., Aghaei, A., 2023. Study of Thermal and Hydrodynamic Performance of a Parabolic Trough Solar Collector Using Hybrid MWCNT/Fe_3O_4-Therminol VP-1 Nanofluid. Energy Eng. Manag. 12, 82–95.

[44] Vahidinia, Farhad, Khorasanizadeh, H., Aghaei, A., 2021. Investigation of energy and exergy performance of parabolic trough solar collector with wind speed variations. J. Aeronaut. Eng. 23, 109–124.

[45] Behar, O., Khellaf, A., Mohammedi, K., 2015. A novel parabolic trough solar collector model–Validation with experimental data and comparison to Engineering Equation Solver (EES). Energy Convers. Manag. 106, 268–281.

[46] Duffie, J.A., Beckman, W.A., Blair, N., 2020. Solar Engineering of Thermal Processes, Photovoltaics and Wind. John Wiley & Sons.

[47] Ekiciler, R., 2024a. Performing SiO_2-MWCNT/water hybrid nanofluid with differently shaped nanoparticles to enhance first-and second-law features of flow by considering a two-phase approach. J. Therm. Anal. Calorim. 149, 1725–1744.

[48] Ekiciler, R., 2024b. Analysis and evaluation of the effects of uniform and non-uniform wall corrugation in a pipe filled with ternary hybrid nanofluid. Arab. J. Sci. Eng. 49, 2681–2694.

[49] Pazarlıoğlu, H.K., Tepe, A.Ü., Tekir, M., Arslan, K., 2022. Effect of new design of elongated jet hole on thermal efficiency of solar air heater. Therm. Sci. Eng. Prog. 36, 101483.

[50] Swinbank, W.C., 1963. Long-wave radiation from clear skies. Q. J. R. Meteorol. Soc. 89, 339–348.

[51] Mullick, S.C., Nanda, S.K., 1989. An improved technique for computing the heat loss factor of a tubular absorber. Sol. Energy 42, 1–7.

[52] Mwesigye, A., Meyer, J.P., 2017. Optimal thermal and thermodynamic performance of a solar parabolic trough receiver with different nanofluids and at different concentration ratios. Appl. Energy 193, 393–413.

[53] Forristall, R., 2003. Heat Transfer Analysis and Modeling of a Parabolic Trough Solar Receiver Implemented in Engineering Equation Solver Heat Transfer Analysis and Modeling of a Parabolic Trough Solar Receiver Implemented in Engineering Equation Solver.

[54] Petela, R., 2003. Exergy of undiluted thermal radiation. Sol. Energy 74, 469–488.

[55] Vahidinia, F., Khorasanizadeh, H., 2024. Comparative energy, exergy and entropy generation study of a minichannel and a conventional solar flat plat collectors. Energy 304, 132232.

[56] Pazarlıoğlu, H.K., Gürsoy, E., Gürdal, M., Said, Z., Arslan, K., Gedik, E., 2024. Numerical simulation of sudden expansion tubes with Ag-MgO nanofluid and innovative fin structure: A thermo-fluidic analysis. Int. J. Heat Fluid Flow 108, 109448.

[57] Bellos, E., Tzivanidis, C., Tsimpoukis, D., 2018. Enhancing the performance of parabolic trough collectors using nanofluids and turbulators. Renew. Sustain. Energy Rev. 91, 358–375.

[58] Malekan, M., Khosravi, A., Syri, S., 2019. Heat transfer modeling of a parabolic trough solar collector with working fluid of Fe_3O_4 and CuO/Therminol 66 nanofluids under magnetic field. Appl. Therm. Eng. 163, 114435.

[59] Ekiciler, R., 2024c. Influence of uniform wall corrugations on convective heat transfer through a convergent–divergent nozzle by using mono and hybrid nanofluids. J. Therm. Anal. Calorim. 149, 1565–1579.

[60] Pazarlıoğlu, H.K., Gürsoy, E., Gürdal, M., Tekir, M., Gedik, E., Arslan, K., Taşkesen, E., 2023b. The first and second law analyses of thermodynamics for $CoFe_2O_4/H_2O$ flow in a sudden expansion tube inserted elliptical dimpled fins. Int. J. Mech. Sci. 246, 108144.

[61] Jasim, L.M., Hamzah, H., Canpolat, C., Sahin, B., 2021. Mixed convection flow of hybrid nanofluid through a vented enclosure with

an inner rotating cylinder. Int. Commun. Heat Mass Transf. 121, 105086.

[62] Ekiciler, R., 2023. Heat transfer enhancement of a slot-confined and submerged impinging jet utilizing lamina-shaped CoFe3O2/water nanofluid. Int. J. Energy Stud. 8, 167–187.

[63] Mwesigye, A., Bello-Ochende, T., Meyer, J.P., 2014. Heat transfer and thermodynamic performance of a parabolic trough receiver with centrally placed perforated plate inserts. Appl. Energy 136, 989–1003.

[64] Bergman, T.L., Lavine, A., Incropera, F.P., Dewitt, D.P., 2017. Fundamentals of heat and mass transfer. John Wiley & Sons New York.

[65] Dudley, V.E., Kolb, G.J., Mahoney, A.R., Mancini, T.R., Matthews, C.W., Sloan, M., Kearney, D., 1994. Test results: SEGS LS-2 solar collector. Sandia National Lab.(SNL-NM), Albuquerque, NM (United States).

[66] Bellos, E., Tzivanidis, C., Antonopoulos, K.A., Gkinis, G., 2016. Thermal enhancement of solar parabolic trough collectors by using nanofluids and converging-diverging absorber tube. Renew. Energy 94, 213–222.

[67] Caliskan, H., 2017. Energy, exergy, environmental, enviroeconomic, exergoenvironmental (EXEN) and exergoenviroeconomic (EXENEC) analyses of solar collectors. Renew. Sustain. Energy Rev. 69, 488–492.